Chapter 2
Fatigue Crack Growth Behaviour of Epoxy Nanocomposites—Influence of Particle Geometry

M.H. Kothmann, G. Bakis, R. Zeiler, M. Ziadeh, J. Breu and V. Altstädt

Abstract In this study, surface-modified spherical nano-silica and K-fluoro hectorites (O/K-hect), characterised by large lateral extensions and aspect ratios, were employed to analyse the effect of geometrical appearance on the fatigue crack growth (FCP) behaviour of an epoxy resin. The addition of nano-silica improved the FCP behaviour by nanoparticle debonding and subsequent plastic void growth. The number of particles contributing to toughening increases remarkably with rising stress intensity factor due to plastic zone enlargement. The improvement in crack propagation resistance by the use of the large O/K-hect, even at very low amounts (2.2 vol%) has to be highlighted. The main toughening mechanism is crack deflection due to the large lateral extension being in the range of the plastic zone size. Especially in the region of crack initiation and stable crack propagation, the clay tactoids reduce the propagation of the damage zone in front of the crack tip remarkably, resulting in a hugely enhanced crack resistance of the nanocomposites.

2.1 Introduction

The long-term mechanical performance under dynamic loading conditions of polymer matrix composites is of prime concern in their adoption for industrial devices. The failure of these composites originates in the formation and subsequent propagation of microcracks. A profound knowledge of the crack propagation behaviour of the polymer matrix material is of fundamental interest. The enhancement of crack resistance by toughening is improving the fatigue performance. The investigation of the fatigue crack propagation (FCP) rate under varying stress intensity ranges (ΔK) allows for a quantification of the three stages of fatigue crack growth: the threshold value for the initiation of fatigue crack growth, the region of stable crack growth, described by the Paris law ((2.1) [1]), and the critical

M.H. Kothmann (✉) · G. Bakis · R. Zeiler · V. Altstädt
Department of Polymer Engineering, University of Bayreuth, Bayreuth, Germany

M. Ziadeh · J. Breu
Department of Inorganic Chemistry, University of Bayreuth, Bayreuth, Germany

W. Grellmann and B. Langer (eds.), *Deformation and Fracture Behaviour of Polymer Materials*, Springer Series in Materials Science 247,
DOI 10.1007/978-3-319-41879-7_2

crack growth. A detailed description of the methodology, as well as a schematic diagram, explaining the different regimes of fatigue crack growth, are given by Fischer et al. [2].

$$\mathrm{d}a/\mathrm{d}N = C \cdot \Delta K^m \tag{2.1}$$

In the Paris law a represents the crack length, N the number of cycles, C a material constant and m the slope of the curve on double logarithmic scale. The plastic zone size, ahead of the crack tip, is strongly dependent on the dynamic stress state applied (2.2) [3]. With increasing stress intensity factor, the size of the plastic zone is enlarged. Consequently, the plastic zone is equivalent to a sensor, changing its size, being highly sensitive to all changes in mechanical properties, attributed to the addition of differently shaped nanoparticles and the crack/particle interactions ahead of the crack tip in the nanocomposites.

$$d_\mathrm{p} = \frac{1}{3\pi}\left(\frac{K_\mathrm{max}}{\sigma_\mathrm{y}}\right)^2 \tag{2.2}$$

According to the crack-tip plasticity theory of Irwin [3], in (2.2), d_p represents the diameter of the plastic zone ahead of the crack tip, K_max the maximum stress intensity factor and σ_y the yield stress of the matrix.

In this work the effect of nanoparticle geometry of non-carbon-based filler materials on the FCP behaviour is focused. Commercial spherical nano-silica (average diameter 20 nm) and surface-modified synthetically prepared K-fluoro hectorites characterised by large lateral extensions (up to 8.6 µm) and high aspect ratios (up to 860) were used to examine the effect of particle size and geometry. The good compatibility of the epoxy resin and silica nanoparticles, due to proper surface treatment, is well known [4]. The fluorohectorites were rendered hydrophobically by cation exchange reaction allowing homogeneous particle dispersion. In addition, the synthetic fluorohectorites provide outstanding advantages compared to natural clays like montmorillonite, including larger particle sizes, superb layer charge homogeneity and high phase purity leading to uniform interlamellar reactivity and surface chemistry [5].

The main toughening mechanisms appearing in epoxy-based silica nanocomposites are particle pull-out in combination with plastic void growth on the nano-level involving slight crack deflection on the micro-level [4]. The lack of crack pinning in epoxy–silica nanocomposites is regarded to be due to the small particle sizes in comparison to the crack-tip-opening displacement, respectively plastic zone size [4, 6]. The morphology of the layered silicates is strongly determined by its degree of exfoliation. On the one hand, the exfoliation of smectite clays is accompanied with a high increase in nanocomposites modulus and tensile strength [7]. Whereas, an increase in fracture toughness is mainly reported for intercalated or phase separated morphologies, especially in the case of mica [8] and modified fluorohectorite [9] filled epoxy systems. As stated by Kinloch and Taylor [8], a certain particle size is necessary to achieve an effective interaction between the

dispersed particles and the propagating crack, by provoking crack deflection and crack pinning. The large fluorohectorites, investigated in this study, provide the opportunity to adjust the particle size and render the state of shear stiffness to improve the load bearing ability in layer stacking direction and the flexural rigidity of the tactoids [5].

Although a lot of effort was spent investigating the mechanical properties of epoxy-based nanocomposites [4, 10, 11], the fatigue crack growth behaviour was less discussed. However, it is described, that for epoxy–silica nanocomposites the stress intensity range required for crack initiation is enhanced [6, 12]. Furthermore, the silica nanoparticles lead to an improved FCP behaviour in all three stages of fatigue crack propagation, while the FCP behaviour of the nanocomposites is systematically improved with increasing amount of nano-silica [6]. Hedicke-Höchstötter et al. [13] observed a significantly improved fatigue crack propagation behaviour of polyamide by adding up to 5 wt% exfoliated layered silicates (Nanofil 919). Although several attempts are presented in literature analysing the effect of specific polymer/nanoparticle combinations in terms of fracture toughness and fatigue crack growth propagation, a comprehensive study discussing the effect of particle geometry of differently shaped nanoparticles in the same resin system is missing. This fact clearly shows the high importance of the presented study to analyse fatigue crack growth behaviour by focusing on particle size and shape and discussing the involved toughening mechanisms.

2.2 Experimental

2.2.1 Materials

The epoxy matrix used in this study consists of a diglycidylether of bisphenol-A (DGEBA) epoxy resin, epoxy equivalent weight 172 g/eq (Epikote resin 0162, Momentive Specialty Chemicals, Germany), cured with methylhexahydrophtalic anhydride (Epikure curing agent 868, Momentive Specialty Chemicals, Germany) and additional 1 wt% N,N′-dimethylbenzyl-amine (Sigma-Aldrich, Germany) referred to the liquid matrix to accelerate curing.

Silica nanocomposites were prepared by using nano-silica, kindly provided as colloidal sol in DGEBA by Evonik Hanse GmbH (Nanopox E470, Evonik-Hanse, Germany, 40 wt% SiO_2). The silica nanoparticles are synthesised and surface-modified, with an organosilane, in aqueous solution. The density of the amorphous nano-silica is approx. 2.2 g cm^{-3} [14].

A synthetic Na-fluorohectorite was prepared by melt synthesis with an optimal chemical formula $Na_{0.5}[Mg_{2.5}Li_{0.5}]Si_4O_{10}F_2$ [15], having a cation exchange capacity (CEC) of 110 meq/100 g as determined by the copper complex method [16]. The aspect ratio of the Na-fluorohectorite was adjusted to maximum 600 and the tactoids were rendered shear stiff by exchanging the intergallery cations with

potassium [5]. Afterwards, the K-fluorohectorites were surface-modified with Dodecylamine (97%, Sigma-Aldrich) using a standard procedure [17]. The density of the organophilised K-fluorohectrite (O/K-hect) is 2.7 g cm^{-3}.

2.2.2 Preparation of Nanocomposites

Epoxy–silica nanocomposites were prepared by simple dilution of the masterbatch with neat DGEBA at 60 °C. Subsequently, the anhydride hardener and the required amount of N,N′-dimethylbenzylamine was added to the mixture.

The epoxy–clay nanocomposites were prepared according to the following procedure. Subsequent to surface modification in aqueous media, the modified fluorohectorites (O/K-hect) were phase transferred into tetrahydrofuran (THF) without former drying by repeated dispersing and centrifuging for two times with THF. As a general procedure, the nanofiller suspension in THF was mixed with the epoxy resin in a round flask for one hour using mechanical mixing. This was followed by removal of the solvent in a rotary evaporator under vacuum at 80 °C. Subsequently, the anhydride hardener was added to the epoxy–nanofiller mixture according to its stoichiometric ratio. The mixture was further processed in a three-roll mill Exakt E80 (Exakt Vertriebs GmbH, Germany) for achieving an optimal dispersion prior to curing (3 cycles, 300 rpm, ultimate gap distance 10 μm). Finally the required amount of N,N′-dimethylbenzylamine was added.

The final mixtures were degassed under vacuum at 60 °C for 15 min and cured at 140 °C for 11 h in a release agent coated aluminium mould.

2.2.3 Characterisation Methods

Powder X-ray diffraction (PXRD) patterns of the final epoxy–clay nanocomposites were recorded to investigate interlamellar spacing of the nanofillers. Samples were fine grinded using cryo-grinding (Pulversiette 14, Fritsch, Germany, 2 mm sieve) and the PXRD patterns were obtained in transmission geometry on a STOE Stadi P powder diffractometer (STOE & Cie GmbH, Germany) equipped with a MYTHEN1K detector using $CuK\alpha_1$ radiation ($\lambda = 0.154056$ nm).

Thermogravimetric analysis (TGA) was applied to determine the amount of the organic modifier of the organo-nanofillers and as well the nanofiller content in the nanocomposites by using a TGA/STDA851e (Mettler Toledo, Germany) under oxygen flow (50 ml/min) at a heating rate of 10 K/min.

The dispersion of the epoxy–silica nanocomposites was characterised using a LEO 922 A energy-filtered transmission electron microscope (EFTEM, Carl Zeiss AG, Germany, 200 kV). Thin sections of 50 nm were cut on a Leica Ultracut microtome (Leica Biosystems GmbH, Germany, 1.5 kV) equipped with a glass knife. Fracture surfaces of selected samples were analysed using a Zeiss 1530 (Carl

Zeiss AG, Germany) scanning electron microscope equipped with a field emission cathode.

Fatigue crack propagation (FCP) experiments were performed at 23 °C and 50% relative humidity employing a servo-hydraulic test machine (Hydropuls MHF, Schenck, Germany) using compact tension (CT) specimens (width 33 mm, thickness 4 mm). The rate of cyclic-fatigue crack growth per cycle, d*a*/d*N*, was measured as a function of the applied stress intensity factor ratio, ΔK. The loading follows a sinusoidal waveform with a frequency of 10 Hz and an *R*-ratio (K_{min}/K_{max}) of 0.1. The calculation of the crack length was done considering the specimen's compliance as described in ISO 15850 [18], using an extensometer (632.13F-20, MTS, Germany) fixed to the front face of the CT specimen.

2.3 Results and Discussion

2.3.1 Organophilisation of Nanoparticles

The amount of surface modifier was determined for the organophilised mica-like fluorohectorite (O/K-hect) using thermogravimetrical analysis. The resulting values as well as the mean particle sizes and aspect ratios are given in Table 2.1. Silica particles were used as received in the DGEBA matrix.

2.3.2 Morphology

The TEM micrographs presented in Fig. 2.1 clearly reveal the homogeneous dispersion of the nano-silica particles. Furthermore, the morphology of the O/K-hect nanocomposites is characterised by the very large fluorohectorite tactoids, well dispersed in the epoxy matrix. Additionally, the high aspect ratio and equal tactoid thickness of the O/K-hect particles are observable. Furthermore, the intergallery distance of the clay tactoids is analysed by using powder X-ray diffraction measurements, revealing no intercalation during dispersion and curing process (Table 2.1). It is noteworthy that O/K-hect particles are modified solely on the external surfaces, since the internal planes are not accessible due to the collapsed structure of the galleries. Consequently, due to the smaller intergallery distance the

Table 2.1 Nomenclature and properties of the different nanofiller employed

Particle	Amount of surface modifier (wt%)	Mean size (nm)	Intergallery distance (nm)	Mean aspect ratio (μm)
Silica	Not determined	20 [4]	- (Amorphous)	1
O/K-hect	4.4	3800	0.99	380

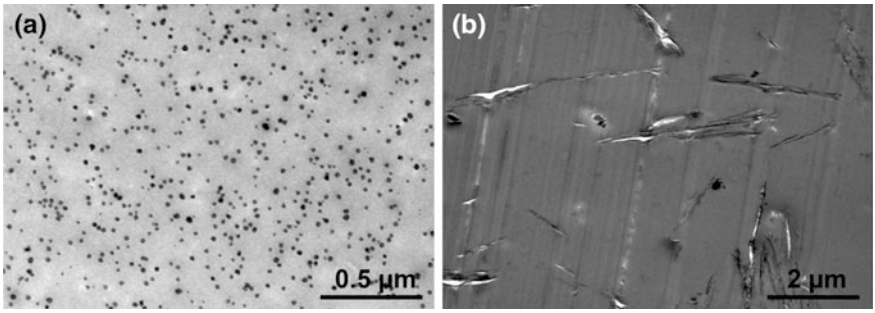

Fig. 2.1 TEM micrographs of the nanocomposites filled with **a** 2.7 vol% SiO_2, and **b** 2.2 vol% O/K-hect

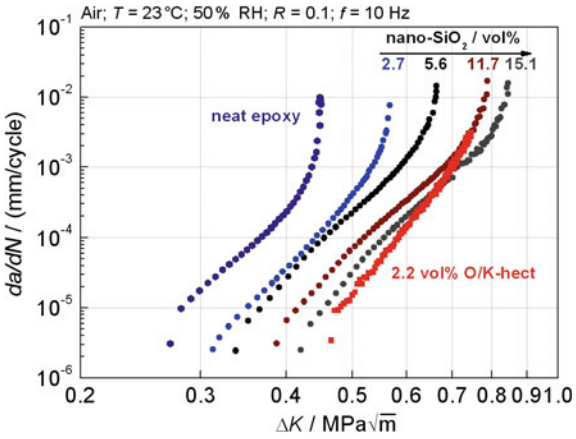

Fig. 2.2 Comparison of the fatigue crack propagation behaviour of nano-silica (2.7–15.1 vol%) and O/K-hect (2.2 vol%) filled epoxy nanocomposites

shear stiffness of O/K-hect is higher as compared to conventional expanded or intercalated organoclays [19].

2.3.3 *Fatigue Crack Propagation Behaviour*

In Fig. 2.2, the effects of spherical nano-silica and layered O/K-hect on the fatigue crack propagation (FCP) behaviour of epoxy nanocomposites is compared.

An improved crack resistance with increasing nano-silica loading is observed in terms of threshold value of crack propagation (ΔK_{th}) and the material behaviour under critical failure (ΔK_{cf}). At 15.1 vol% an improvement of 66% in ΔK_{th} and 88% in ΔK_{cf}, is obtained. The fracture surfaces of the nanocomposite containing

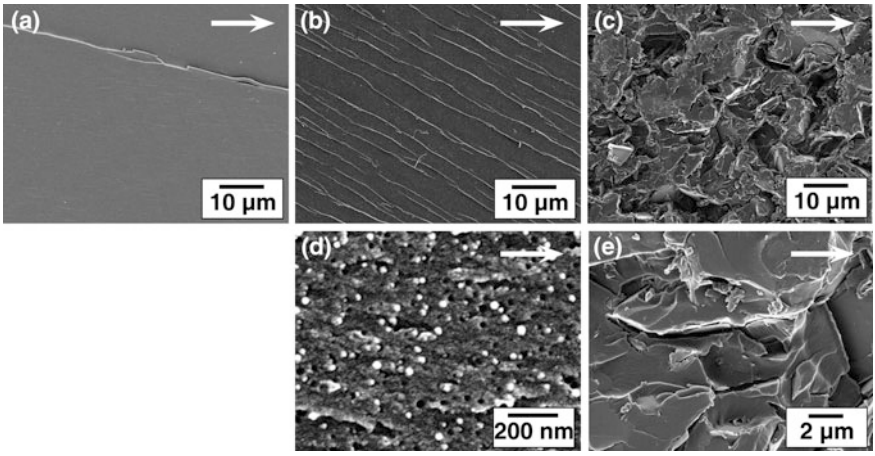

Fig. 2.3 Fracture surfaces (SEM) of the different nanocomposites in the region of stable crack growth, **a** neat epoxy, **b** and **d** nano-SiO_2 nanocomposites, **c** and **e** O/K-hect nanocomposites. The direction of crack propagation is indicated by the *white arrows*

5.6 vol% nano-silica (Fig. 2.3b, d; for the neat epoxy see Fig. 2.3a) reveal particle debonding and plastic void growth as the main toughening mechanisms, combined with an enhanced shear yielding of the matrix. According to the model of Irwin [3], describing the increasing diameter of the cylindrically shaped plastic zone (d_p) with respect of ΔK, respectively K_{max} [$d_p \sim \Delta K^2$, (2.2)], the number of silica nanoparticles (n) contributing to toughening increases. The number of silica nanoparticles within the plastic zone follows a power law with the exponent of 4 ($n \sim \Delta K^4$), being reflected in the more pronounced FCP improvement at higher crack propagation rates. This is also reflected in the reduction of the slope (m) in the Paris regime (2.1). A detailed description of this correlation is given in [6].

In addition a pronounced improved crack resistance is observed for the O/K-hect–epoxy nanocomposite even at very low amounts of nanofiller. The characteristic values ΔK_{th} and ΔK_{cf} are improved by 73 and 67% by adding 2.2 vol% O/K-hect. The fracture surfaces (Fig. 2.3c, e) of the nanocomposite (2.2 vol% O/K-hect) reveal a very tortious fracture surface, attributed to strong crack deflection and crack pinning, provoked by the large lateral particle size. Obviously, on a microscopic scale the crack is forced to propagate along the interface between the epoxy resin and the clay tactoids (particle debonding). As a consequence of the specific orientation and the high aspect ratio of the clay tactoids, the crack is deflected locally, increasing the crack path length and leading to an enlargement in the newly formed fracture surface (Fig. 2.3e). Particle cleavage was not observed since the filler–matrix adhesion is regarded being moderate, since the aliphatic dodecyl-tails of the surface modifier show neither entanglements, nor form any covalent crosslinking with the thermosetting matrix.

Comparing the nanocomposites containing comparable nanofiller contents (2.7 vol% nano-silica respectively 2.2 vol% O/K-hect) the dependency of the FCP behaviour on the stress intensity of the nano-silica and the O/K-hect nanocomposites, as expressed by the shape of the FCP curves, is similar. Although the toughening potential of the larger O/K-hect is more prominent, since ΔK_{th} and ΔK_{cf} are improved more significantly. Estimating and comparing the number of particles and their corresponding particle surface area in a reference volume, using the geometrical parameters of the fillers (Table 2.1) reveals a much higher number (33,000×) and surface area (1.5×) in the case of nano-silica as compared to O/K-hect. Despite the lower number of particles and surface area, the toughening effect is more pronounced in the case of O/K-hect. Leading to the conclusion, toughening dominated by crack deflection as in the case of O/K-hect is more effective as compared to particle debonding, in the case of nano-silica.

In the region of unstable crack growth (ΔK_{cf}), the addition of 11.7 vol% nano-silica exhibits a crack resistance improvement, being comparable to the addition of 2.2 vol% of O/K-hect. Whereas the toughening efficiency of the nano-silica is less pronounced in the region of crack initiation (ΔK_{th}) and stable crack propagation (Paris regime). This phenomenon, accessible by fatigue crack growth experiments cannot be observed by quasi-static fracture toughness experiments investigating solely critical crack growth. In the region of crack initiation, the diameters of the plastic zones, determined according to the theory of Irwin ((2.2), σ_y = 82 MPa), are approx. 2 and 4 μm in the case of nano-silica (11.7 vol%) and O/K-hect (2.2 vol%) respectively. Due to the large average lateral extension of the O/K-hect (4 μm), the plastic zone can be completely spanned by a single tactoid, decelerating the propagation of the damage zone at the crack tip. Additionally, for complete debonding of an O/K-hect, multiple fatigue cycles are necessary, since the crack propagation per cycle (da/dN) is in the sub-micron range. At higher ΔK, i.e. with increasing plastic zone size, several O/K-hect particles are required for effective crack deflection. Whereas in the case of nano-silica, the effectivity of debonding is multiplied due to the tremendously increased number of particles in the enlarged plastic zone, contributing to toughness enhancement by debonding. These mechanisms clearly explain the distinctive dependencies on ΔK (stages of fatigue crack growth) applied towards the enhancement of crack resistance of the nanofillers, possessing variations in the geometry.

2.4 Conclusion

In this study, surface-modified spherical nano-silica and K-fluorohectorites (O/K-hect), characterised by large lateral extensions and aspect ratios, were employed to analyse the effect of geometrical appearance on the fatigue crack growth (FCP) behaviour of an epoxy resin. The addition of nano-silica improved the FCP behaviour by nanoparticle debonding and subsequent plastic void growth. The number of particles contributing to toughening increases remarkably with

rising ΔK due to plastic zone enlargement. The improvement in crack propagation resistance by the use of the large O/K-hect, even at very low amounts (2.2 vol%) has to be highlighted. The main toughening mechanism is crack deflection due to the large lateral extension being in the range of the plastic zone size. Especially in the region of crack initiation and stable crack propagation, the clay tactoids reduce the propagation of the damage zone in front of the crack tip remarkably, resulting in a hugely enhanced crack resistance of the nanocomposites.

Acknowledgements The authors highly acknowledge the financial support from the German Research Foundation in the frame of the Collaborative Research Center SFB 840: "From particulate nanosystems to mesotechnology", and from the German Federal Ministry for Economic Affairs and Energy (FKZ 0327895E). The authors are grateful towards Mr. Brückner, Mrs. Lang, and Mrs. Förtsch, University of Bayreuth, for their support with the mechanical characterisation and microscopic investigations, respectively.

References

1. Paris, P., Erdogan, F.: A critical analysis of crack propagation laws. J. Basic Eng. **85**, 528–533 (1963)
2. Fischer, F., Beier, U., Wolff-Fabris, F., Altstädt, V.: Toughened high performance epoxy resin system for aerospace applications. Sci. Eng. Compos. Mater. **18**, 209–215 (2011)
3. Kinloch, A.J., Young, R.J. (eds.): Fracture Behaviour of Polymers. Applied Science Publishers, London (1983)
4. Johnsen, B.B., Kinloch, A.J., Mohammed, R.D., Taylor, A.C., Sprenger, S.: Toughening mechanisms of nanoparticle-modified epoxy polymers. Polymer **48**, 530–541 (2007)
5. Möller, M.W., Handge, U.A., Kunz, D.A., Lunkenbein, T., Altstädt, V., Breu, J.: Tailoring shear-stiff, mica-like nanoplatelets. ACS Nano **4**, 717–724 (2010)
6. Kothmann, M.H., Zeiler, R., Rios de Anda, A., Brückner, A., Altstädt, V.: Fatigue crack propagation behaviour of epoxy resins modified with silica-nanoparticles. Polymer **60**, 157–163 (2015)
7. Shi, H., Lan, T., Pinnavaia, T.J.: Interfacial effects on the reinforcement properties of polymer–organoclay nanocomposites. Chem. Mater. **8**, 1584–1587 (1996)
8. Kinloch, A.J., Taylor, A.C.: The mechanical properties and fracture behaviour of epoxy-inorganic micro- and nano-composites. J. Mater. Sci. **41**, 3271–3297 (2006)
9. Kornmann, X., Thomann, R., Mülhaupt, R., Finter, J., Berglund, L.: Synthesis of amine-cured, epoxy-layered silicate nanocomposites: the influence of the silicate surface modification on the properties. J. Appl. Polym. Sci. **86**, 2643–2652 (2002)
10. Dittanet, P., Pearson, R.A.: Effect of silica nanoparticle size on toughening mechanisms of filled epoxy. Polymer **53**, 1890–1905 (2012)
11. Zhang, H., Zhang, Z., Friedrich, K., Eger, C.: Property improvements of in situ epoxy nanocomposites with reduced interparticle distance at high nanosilica content. Acta Mater. **54**, 1833–1842 (2006)
12. Blackman, B.R.K., Kinloch, A.J., Lee, J.S., Taylor, A.C., Agarwal, R., Schueneman, G., Sprenger, S.: The fracture and fatigue behaviour of nano-modified epoxy polymers. J. Mater. Sci. **42**, 7049–7051 (2007)
13. Hedicke-Höchstötter, K., Demchuk, V., Langenfelder, D., Altstädt, V.: Fatigue crack propagation behaviour of polyamide-6 nanocomposites based on layered silicates. J. Plast. Technol. **3**, 1–22 (2007)

14. Tang, L.-C., Zhang, H., Sprenger, S., Ye, L., Zhang, Z.: Fracture mechanisms of epoxy-based ternary composites filled with rigid-soft particles. Compos. Sci. Technol. **72**, 558–565 (2012)
15. Kalo, H., Möller, M.W., Ziadeh, M., Dolejš, D., Breu, J.: Large scale melt synthesis in an open crucible of Na-fluorohectorite with superb charge homogeneity and particle size. Appl. Clay Sci. **48**, 39–45 (2010)
16. Ammann, L., Bergaya, F., Lagaly, G.: Determination of the cation exchange capacity of clays with copper complexes revisited. Clay Miner. **40**, 441–453 (2005)
17. Carrado, K.A., Decarreau, A., Petit, S., Bergaya, F., Lagaly, G.: Synthetic clay minerals and purification of natural clay. In: Bergaya, F., Theng, B.K.G., Lagaly, G. (eds.) Handbook of Clay Science, pp. 115–139. Elsevier, Amsterdam (2006)
18. ISO 15850 (2014): Plastics—Determination of tension-tension fatigue crack propagation—Linear elastic fracture mechanics (LEFM) approach
19. Stefanescu, E.A., Tan, X., Lin, Z., Bowler, N., Kessler, M.R.: Multifunctional PMMA–ceramic composites as structural dielectrics. Polymer **51**, 5823–5832 (2010)

http://www.springer.com/978-3-319-41877-3

Deformation and Fracture Behaviour of Polymer Materials

Grellmann, W.; Langer, B. (Eds.)
2017, XXXII, 533 p. 328 illus., 219 illus. in color., Hardcover
ISBN: 978-3-319-41877-3